JOURNAL OF BACTERIOLOGY, June 2005, p. 4064–4076 Vol. 187, No. 12
0021-9193/05/$08.00+0 doi:10.1128/JB.187.12.4064–4076.2005

A VicRK Signal Transduction System in *Streptococcus mutans* Affects *gtfBCD*, *gbpB*, and *ftf* Expression, Biofilm Formation, and Genetic Competence Development

M. Dilani Senadheera,[1] Bernard Guggenheim,[2] Grace A. Spatafora,[3] Yi-Chen Cathy Huang,[1] Jison Choi,[4] David C. I. Hung,[4] Jennifer S. Treglown,[4] Steven D. Goodman,[4] Richard P. Ellen,[1] and Dennis G. Cvitkovitch[1]*

Dental Research Institute, University of Toronto, 124 Edward Street, Toronto, Ontario M51G6, Canada[1]; Institute for Oral Biology, Section for Oral Microbiology and General Immunology, Center for Dental, Oral Medicine and Maxillofacial Surgery, University of Zurich, Zurich, Switzerland[2]; Department of Biology, Middlebury College, 276 Bicentennial Way, BIH354, Middlebury, Vermont 05753[3]; and Division of Diagnostic Science, Norris School of Dentistry, University of Southern California, 925 West 34th, Los Angeles, California 90089[4]

Received 19 November 2004/Accepted 9 March 2005

Bacteria exposed to transient host environments can elicit adaptive responses by triggering the differential expression of genes via two-component signal transduction systems. This study describes the *vicRK* signal transduction system in *Streptococcus mutans*. A *vicK* (putative histidine kinase) deletion mutant (SmuvicK) was isolated. However, a *vicR* (putative response regulator) null mutation was apparently lethal, since the only transformants isolated after attempted mutagenesis overexpressed all three genes in the *vicRKX* operon (Smuvic$^+$). Compared with the wild-type UA159 strain, both mutants formed aberrant biofilms. Moreover, the *vicK* mutant biofilm formed in sucrose-supplemented medium was easily detachable relative to that of the parent. The rate of total dextran formation by this mutant was remarkably reduced compared to the wild type, whereas it was increased in Smuvic$^+$. Based on real-time PCR, Smuvic$^+$ showed increased *gtfBCD*, *gbpB*, and *ftf* expression, while a recombinant VicR fusion protein was shown to bind the promoter regions of the *gtfB*, *gtfC*, and *ftf* genes. Also, transformation efficiency in the presence or absence of the *S. mutans* competence-stimulating peptide was altered for the *vic* mutants. In vivo studies conducted using SmuvicK in a specific-pathogen-free rat model resulted in significantly increased smooth-surface dental plaque (Pearson-Filon statistic [PF], <0.001). While the absence of *vicK* did not alter the incidence of caries, a significant reduction in SmuvicK CFU counts was observed in plaque samples relative to that of the parent (PF, <0.001). Taken together, these findings support involvement of the *vicRK* signal transduction system in regulating several important physiological processes in *S. mutans*.

Among the hundreds of bacterial species that colonize and persist in the oral cavity, *Streptococcus mutans* is among the few species that have been consistently linked with caries formation (31). Under the low-pH conditions that define the plaque environment, *S. mutans* induces an acid tolerance response that helps it survive (14, 15, 18). Hence, the ability to adapt to and generate acids at the tooth surface allows *S. mutans* to predominate within carious lesions by reducing the plaque pH to levels that are inhibitory to other oral microbes (34, 47). In addition, the ability of *S. mutans* to synthesize extracellular polysaccharides that promote formation of the plaque biofilm also contributes to its pathogenicity (35, 47). As a result, investigations to characterize virulence determinants of this oral pathogen have continued to dominate the caries microbiology field for decades.

Two-component signal transduction systems (TCSTS) are among the regulatory networks that are essential for bacterial adaptation, survival, and virulence. These systems function as "molecular switches" to modulate gene expression in response to changes in the external environment (44). Typically, signal transduction is accomplished via two regulatory elements consisting of a membrane-associated histidine kinase and a cytoplasmic response regulator. Upon exposure to an environmental cue, such as pH, osmolarity, or oxidation-reduction potential, the histidine kinase becomes autophosphorylated at a conserved histidine residue. Following the transfer of this phosphate group to a response regulator, the regulator can control the transcription of target genes by binding to their promoter regions. Diverse metabolic processes controlled by TCSTS include chemotaxis, sporulation, quorum sensing, and antibiotic/bacteriocin production in a wide variety of bacteria (3, 8, 30, 43, 45). Previous work conducted in one of our laboratories indicated that genetic competence, biofilm formation, and acid tolerance are mediated by detection of a signal peptide by the *comDE* TCSTS in *S. mutans* (27, 28). Genetic competence enables recipient bacteria to inherit heterologous genes that can contribute to the emergence of antibiotic resistance, as well as promote genetic variation that can drive overall fitness and evolution (7).

Analysis of the *S. mutans* UA159 genome database revealed 13 putative TCSTS and at least one independent response regulator (1, 21). The present study describes an investigation into the *S. mutans vicRK* signal transduction system that en-

* Corresponding author. Mailing address: Rm. 449A, Dental Research Institute, 124 Edward Street, Toronto ON M51G6, Canada. Phone: (416) 979-4917, ext. 4592. Fax: (416) 979-4936. E-mail: dennis.cvitkovitch@utoronto.ca.

A

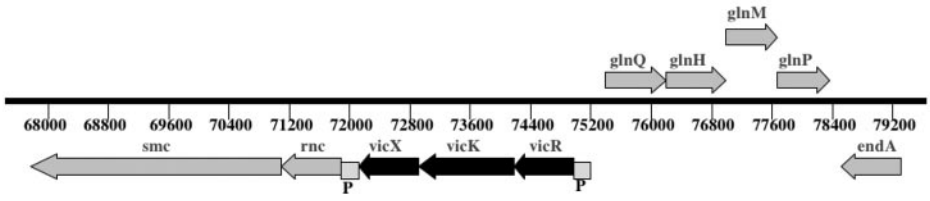

B

	Bs YycF	*Sp* CovR	*Sp* VicR	*Sm* CovR (VicR)	*Sa* VicR
***Sm* CovR (VicR)**	71[a], 81[b]	43, 59	90, 93	-	64, 80
***Bs* YycF**	-	45, 63	70, 82	71, 81	75, 89
***Spn* YycF**	67,79	45, 67	78, 89	78, 89	62, 89
***Sp* CovR**	45, 63	-	40, 58	43, 59	40, 62
***Sp* VicR**	70, 82	40, 58	-	90, 93	63, 82
***Sm* GcrR**	44, 59	75, 84	41, 59	42, 59	40, 61

Note: Percentage identity (a), percentage similarity (b).

FIG. 1. (A) Genetic map of the *vicRKX* operon. Using BlastP searches, putative functions were assigned to genes based on high identity scores in the NCBI website. Abbreviations: smc, chromosome segregation SMC protein in *Streptococcus agalactiae* (accession no. NP_687739.1); rnc, RNase III in *S. agalactiae* (NP_687738.1); vicX, *S. pyogenes* VicX protein (NP_268804.1), VicX protein in *S. pneumoniae* (NP_345691.1), and metallo-β-lactamase superfamily protein in *S. agalactiae* (NP_687736.1); vicK, *S. pyogenes* VicK histidine kinase sensor protein (NP_268803.1), VicK in *S. pneumoniae* (NP_268803), and a sensory box histidine kinase in *S. agalactiae* (NP_687735.1); vicR, *S. pyogenes* VicR response regulator protein (NP_268802.1) and in *S. pneumoniae* (NP_606786.1); glnQ to glnP, glutamine transport ATP-binding protein (NP_687733.1), glutamine binding protein (NP_687732.1), amino acid permease protein (NP_687731.1), and integral membrane protein (NP_687730.1) in *S. agalactiae*, respectively; endA, putative membrane nuclease EndA in *S. pneumoniae* (NP_359371.1). (B) BlastP search results using the NCBI website and comparing various VicR and CovR proteins from various microorganisms (*Spn*, *S. pneumoniae*; *Sm*, *S. mutans*; *Sp*, *S. pyogenes*; *Sa*, *S. aureus*; *Bs*, *B. subtilis*).

codes a putative histidine kinase (VicK) and a response regulator (VicR) (Fig. 1A). This TCSTS in *S. mutans* was first described as *covRS* by Lee et al. (GenBank accession number AF393849), after its homolog in *Streptococcus pyogenes* (26). While this system does bear sequence similarity to the *covRS* system of *S. pyogenes*, it appears more closely related to the *vicRK* TCSTS of *S. pyogenes* and *Streptococcus pneumoniae*. To clarify this further, the *S. pyogenes covR* homolog in *S. mutans* was named *gcrR* by Sato et al. (40) and later renamed *tarC* following its characterization by Idone et al. (21). Figure 1B clarifies the relationship between various members of these TCSTS families. Based on these observations, it seems more appropriate to refer to this TCSTS as *vicRK* as previously named in the annotated *S. mutans* UA159 genome sequence available in the National Center for Biotechnology Information (NCBI) GenBank database (1). In this paper, we chose to henceforth refer to the TCSTS as *vicRK* in accordance with its designation by Ajdic et al. (1).

The *vicRK* TCSTS family is best characterized in *S. pneumoniae* and in *Bacillus subtilis* (10, 12, 20, 46). In a study conducted by Wagner et al., overexpression of the *vicK* gene in *S. pneumoniae* resulted in a mutant attenuated for virulence in a mouse model (46). Also, a *vicK* null mutant demonstrated a decrease in transformation efficiency (TE) relative to the wild type by approximately 3 orders of magnitude (46). Efforts to generate a deletion mutation in the *S. pneumoniae vicR* ho-

TABLE 1. Bacterial strains, plasmids, and amplicons used in this study

Strain, plasmid, or amplicon	Relevant characteristic(s)	Source or reference
S. mutans strains		
UA159	Wild type	A. S. Bleiweis, University of Florida
SmuvicK	UA159 *vicK*::*ermAM* Erm	This study
Smuvic$^+$	UA159 derived; *vicRKX* overexpression; Erm^r	This study
Plasmids		
pDL277	*E. coli*-streptococcal shuttle vector; Spec^r	4
pMal-c2	*E. coli* expression vector with MBP; Amp^r	New England Biolabs
pSG385	*E. coli* pMal-c2 containing VicR; Amp^r	This study
Amplicons		
PcErm	Erm^r marker amplified using *ermAM* cassette	
aVicK	*vicK*-5′::PcErm::*vicK*-3′ fragment used for allelic replacement of *vicK* gene	This study
aVicR	*vicR*-5′::PcErm::*vicR*-3′ fragment used for allelic replacement of *vicR* gene	This study

molog (*vicR*), however, proved unsuccessful. In contrast to the recent publication by Lee et al. (26), in this study we claim that *vicR* inactivation in *S. mutans* is also lethal. Herein we describe a link between *vicRK* signal transduction and *S. mutans* sucrose-dependent adhesion, biofilm formation, and competence development. We also report our assessment of the abilities of an *S. mutans vicK*-deficient mutant to form plaque and generate caries in a specific-pathogen-free rat model.

MATERIALS AND METHODS

Bacterial strains, plasmids, and media. The bacterial strains, plasmids, and amplicons used in this study are listed in Table 1. The *S. mutans* UA159 wild-type strain and its derivatives were routinely maintained on Todd-Hewitt yeast extract (THYE) agar (BBL Becton Dickinson, Cockeysville, MD) containing appropriate antibiotics when needed. Antibiotics used for the mutant strains were erythromycin (10 μg/ml), spectinomycin (1,200 μg/ml), kanamycin (500 μg/ml), and tetracycline (10 μg/ml). All *S. mutans* cultures were routinely grown as standing cultures at 37°C in a 5% CO_2–95% air mixture.

Construction of *S. mutans vicRK* mutants. We searched the *S. mutans* UA159 genome database (http://www.genome.ou.edu/smutans.html) for *vicR* and *vicK* homologs using the *S. pneumoniae* RR02 and HK02 amino acid sequences as queries, respectively. To delete the *vicRK* gene pair in *S. mutans* UA159, we used a ligation-PCR mutagenesis strategy as previously described (25). The resulting putative histidine kinase mutant was termed SmuvicK, while repeated attempts to generate a *vicR* null mutant in the NG8 and UA159 backgrounds proved to be futile. In the latter case, all recovered transformants overexpressed the *vicRKX* genes and were hence designated Smuvic$^+$. The primers used for mutant construction and confirmation are listed in Table 2. Ligation constructs were introduced into *S. mutans* by competence-stimulating peptide (CSP)-induced natural transformation (28), and transformants resistant to erythromycin were selected to confirm appropriate recombination into the chromosome by PCR, followed by nucleotide sequence analysis. The *vicRKX* expression in the resulting mutants was monitored using quantitative real-time PCR (rtPCR) and compared with expression in the UA159 wild-type progenitor.

Growth rates. Growth kinetics were monitored using a Bioscreen microbiology reader (Bioscreen C Labsystems, Helsinki, Finland). Overnight cultures were diluted 20× in fresh THYE and grown to an optical density at 600 nm (OD_{600}) of approximately 0.4 to 0.5. Twenty microliters of mid-log-phase cells for the mutant and wild-type strains were inoculated in triplicate into microtiter plate wells containing 400 μl of THYE. Wells containing uninoculated THYE were used as controls. Using Biolink software (Labsystems), the Bioscreen reader was programmed to monitor OD_{600}s at 37°C every 20 min for 24 h, with moderate shaking every 3 min. OD_{600} measurements were plotted against time to generate growth curves.

***S. mutans* biofilm formation.** A modified semidefined minimal medium (SDM) was prepared for biofilm growth experiments as described previously (29, 32). Biofilms were formed in 24-well polystyrene microtiter plates containing 2 ml of medium supplemented with 20 mM glucose or 10 mM sucrose. All wells were inoculated with 20 μl of an overnight cell suspension. In addition to SDM, SmuvicK and UA159 biofilms were also formed in 0.25× THYE that was supplemented with 20 mM glucose or 10 mM sucrose. Following incubation at 37°C and 5% CO_2 for 16 h, the broth was gently removed by aspiration and the biofilms photographed directly. To closely examine the architecture of the parent and mutant biofilms, we utilized scanning electron microscopy (SEM) as described previously (28).

RNA preparation and rtPCR analysis. To measure *gtfB*, *gtfC*, and *ftf* expression, total RNA was isolated from bacterial cultures grown in Tryptone yeast extract broth supplemented with 1% sucrose or 1% glucose. To study *vicRK* expression, bacterial strains were grown in THYE with or without antibiotics. Overnight cultures were diluted 20× in fresh broth and then grown to mid-logarithmic phase. Cells were harvested by centrifugation and immediately resuspended in Trizol reagent (Invitrogen) prior to RNA isolation using the FastPrep system (Bio 101 Savant) as specified by the manufacturer. To monitor gene expression, total RNA was subjected to DNase treatment and then reverse transcribed using a first-strand cDNA synthesis kit (MBI Fermentas) in accordance with the recommendations of the supplier. Controls for cDNA synthesis included a condition with no RNA template and another without reverse transcriptase. Finally, the single-stranded cDNAs were incorporated into rtPCR experiments using a Cepheid Smart Cycler system (Cepheid, Sunnyvale, CA) and a Quantitect SYBR-Green PCR kit (QIAGEN). Each 25-μl reaction mixture included template cDNA, 25 μM each primer, and 2× SYBR-Green mix (containing SYBR-Green, deoxynucleoside triphosphates, $MgCl_2$, and Hotstar *Taq* polymerase). For maximum efficiency, rtPCR primers were designed to generate amplicons ranging from 100 to 170 bp in size (Table 2). Controls for rtPCR included reaction mixtures without template cDNA to effectively rule out the presence of contaminating DNA and/or the formation of primer dimers. The cycling conditions were as follows: 95°C for 15 min for the initial denaturation, followed by 35 to 40 cycles of three steps consisting of denaturation at 94°C for 15 s, primer annealing at the optimal temperature (Table 2) for 30 s, and primer extension at 72°C for 30 s. For each set of primers, cycle threshold (Ct) values, defined as the first cycle that gave rise to a detectable PCR product above the background, were generated. Known genomic DNA concentrations were used to generate Ct values for specific primer sets. By plotting the DNA concentrations versus the Ct value, standard curves were generated and used to determine relative RNA expression levels for the test gene. Results were normalized against *S. mutans gyrA* expression that was invariant under the experimental test conditions.

Purification of MBP-VicR. The *vicR* coding sequence was amplified by PCR using chromosomal DNA derived from *S. mutans* UA159 with primers oSG241 and oSG242. Subsequently, the amplicon was digested with HindIII and EcoRI and ligated to maltose-binding protein (MBP) expression vector pMalc2 (New England Biolabs, Beverly, MA). The resulting plasmid, pSG385, was introduced into *Escherichia coli* strain TB1 and selected for resistance to ampicillin. For overexpression, *E. coli* strain TB1 cells containing pSG385 were grown in 1 liter of LB supplemented with 2% glucose and 100 μg/ml ampicillin at 37°C with shaking. When cells reached an OD_{600} of 0.3 to 0.5, expression of the MBP fused to VicR (MBP-VicR) was induced with 0.3 mM isopropyl-β-D-thiogalactopyranoside (IPTG) for 2 h. The cells were harvested by centrifugation (4°C, 5,000 × *g*, 15 min), resuspended in column buffer (20 mM Tris-HCl, pH 7.4, 200 mM NaCl, 1 mM EDTA), frozen at −20°C overnight, and lysed by sonication. Cells

TABLE 2. Primers used for PCR-ligation mutagenesis, rtPCR, VicR cloning, and mobility shift experiments

Primer use and name	Nucleotide sequence[d]	Annealing temp (°C), size (bp)
PCR-ligation mutagenesis[a]		
VicK-P1	5′ TGGTAAAGCAGTATCTGGCGAGG 3′	53.1, 666
VicK-P2	5′ **GG^CGCGCC**ATAGTGAGGAAGGCGAAGGGTC 3′	
VicK-P3	5′ **GGCCGG^CCC**CAGGGACTTGATTCAAACACATTAG 3′	54.1, 886
VicK-P4	5′ GGCTAAGGAAGGTTATGACACG 3′	
VicR-P1	5′ TCTTTTTCCTGTTCGGTCG 3′	51.4, 615
VicR-P2	5′ **GG^CGCGCC**GATGTTACTGTTCGTCGTCTGC 3′	
VicR-P3	5′ **GGCCGG^CCC**CGTGTCATAACCTTCCTTAGCCA 3′	51.5, 711
VicR-P4	5′ AGTTCACCAGAGTCAATGGATTCC 3′	
Erm cst-F	5′ **GG^CGCGCC**CCGGGCCCAAAATTTGTTTGAT 3′	52.3, 876
Erm cst-B	5′ **GGCCGG^CC**AGTCGGCAGCGACTCATAGAAT 3′	
rtPCR primers		
VicK-FOR	5′CACTTTACGCATTCGTTTTGCC 3′	52.0, 102
VicK-REV	5′ CGTTCTTCTTTTTCCTGTTCGGTC 3′	
VicR-FOR	5′ CGCAGTGGCTGAGGAAAATG 3′	53, 157
VicR-REV	5′ ACCTGTGTGTGTCGCTAAGTGATG 3′	
VicX-FOR	5′ TGCTCAACCACAGTTTTACCG 3′	51.4, 127
VicX-REV	5′ GGACTCAATCAGATAACCATCAGC 3′	
Ftf-FOR	5′ ATTGGCGAACGGCGACTTACTC 3′	52.8, 103
Ftf-REV	5′ CCTGCGACTTCATTACGATTGGTC 3′	
GtfB-FOR	5′ ACACTTTCGGGTGGCTTG 3′	49, 127
GtfB-REV	5′ GCTTAGATGTCACTTCGGTTG 3′	
GtfC-FOR	5′ CCAAAATGGTATTATGGCTGTCG 3′	50.5, 136
GtfC-REV	5′ TGAGTCTCTATCAAAGTAACGCAG 3′	
GyrA-FOR	5′ ATTGTTGCTCGGGCTCTTCCAG 3′	62.0, 105
GyrA-REV	5′ ATGCGGCTTGTCAGGAGTAACC 3′	
VicR cloning[b]		
oSG241	5′ CCG**gaattc**TATTTTAAGACCATAAGCGAGGTA 3′	
oSG242	5′ CCC**aagctt**GCTAATAAAATTCGTAAAAATAAGGGAC 3′	
Mobility shift products[c]		
oSG64 (*gtfB*)	5′ *GGATATCCC*ATGGTAGGAACCTCCAAATTTTAAACTG 3′	
oSG181 (*gtfC*)	5′ AGATACTGTCACCCATCTTTT 3′	
oSG258 (*ftf*)	5′ CCACCCAAAATTTCCCTTTC 3′	
oSG264 (*gtfB*)	5′ CAATTAGACTGTTGTTTTTTTG 3′	
oSG137 (*gtfC*)	5′ *CGGGATCC*ATTTATTATTTTTCTAAAAAA 3′	
oSG265 (*ftf*)	5′ CTTAATCTAATATGTGAATTTGTT 3′	

[a] AscI restriction sites are in boldface, and FseI restriction sites are underlined.
[b] HindIII cut site is in boldface, and EcoRI cut site is in boldface and underlined.
[c] Underlined italics indicate linker bases.
[d] Circumflexes indicate restriction enzyme cleavage sites.

that were not lysed along with other debris were removed by centrifugation (9,000 × *g*, 20 min, 4°C). The cleared cell lysate was applied to an amylose resin column (New England Biolabs), preequilibrated with column buffer, and then washed with 12 column volumes of column buffer. The protein was eluted with column buffer containing 10 mM maltose. Three-milliliter fractions were collected, and fractions containing MBP-VicR, as determined by sodium dodecyl sulfate-polyacrylamide gel electrophoresis, were pooled and concentrated using an Amicon Ultra-15 concentrator (Millipore, Billerica, MA). Briefly, fractions containing MBP-VicR were applied to the filter device and centrifuged at 3,000 × *g* and 4°C for 15 min. To reduce the salt concentration, the filter was washed with modified column buffer (20 mM Tris-HCl, pH 7.4, 50 mM NaCl, 1 mM EDTA) and the purified protein was concentrated to ~2 ml. The concentration of MBP-VicR was determined by using the Bio-Rad Protein Assay (Bio-Rad, Hercules, CA) using bovine serum albumin as the standard. The purified protein was stored at 4°C or in glycerol at −80°C until needed.

Mobility shift experiments. The primers oSG181, oSG258, and oSG64 were end labeled by incubating 1 μM primer with 1 μM [γ-^{32}P]ATP, 0.5 μM unlabeled ATP, T4 polynucleotide kinase (Promega, Madison, WI), and 1× polynucleotide kinase buffer at 37°C for 30 min. The labeled oSG181 primer was then used to generate a 194-bp *gtfC* promoter-containing fragment using oSG137. The labeled oSG258 primer was then used to generate a 215-bp *ftf* promoter-containing fragment using oSG265. Labeled primer oSG64 and unlabeled primer oSG264 were used to generate a 205-bp *gtfB* promoter-containing fragment. For the binding reactions, the labeled *gtfB* (−159 to +36), *gtfC* wild-type (−89 to +102), and *ftf* (−141 to +74) promoter-containing fragments were incubated at room temperature for 30 min with 0 to 1,000 nM MBP-VicR, reaction buffer (52.5 mM MOPS pH 7.4, 9.5% glycerol, 50 μM EDTA, 50 μg/ml bovine serum albumin), and 50 ng salmon sperm DNA in a volume of 20 μl. Protein-DNA complexes were separated by nondenaturing gel electrophoresis on 6% acrylamide gels at 10 V/cm for 3 h, dried, and visualized with a phosphorimager.

Extracellular polysaccharide synthesis (EPS). Cell cultures at mid-logarithmic phase derived from 1:20 dilutions of overnight cultures were centrifuged for 10 min at 4,500 rpm. To measure "released" activity in the culture fluid, the supernatants were filter sterilized and stored at −20°C until further use. EPS assays were conducted by adding 50 μl of a buffer mixture (100 mM sodium acetate buffer [pH 5.5], 7 mM sodium fluoride, 0.02% dextran T-10 [average weight, 10,000]) to 200 μl of cell-free supernatants. Following their incubation at 37°C for 10 min, 0.6 mM [^{14}C]sucrose (11 μCi/μmol) was added to the mixtures, which were then vortexed, and 15 μl of each mixture was spotted in triplicate onto 2.3-cm square Whatman 3 MM filter papers. This procedure was repeated after mixtures were incubated at 37°C for 30 min. Subsequently, the filter papers were washed three times, 15 min each, in methanol using at least 10 ml of solvent. Filter squares were then dried and radioactivity counted using a liquid scintillation counter. Net EPS activity was measured as the difference in counts at $t = 30$ and $t = 0$.

Competence assay. Overnight cultures of SmuvicK, Smuvic$^+$, and their UA159 parent were diluted 20- or 40-fold in prewarmed THYE and incubated at 37°C until an OD_{600} of approximately 0.3 was reached. Following the incubation period, 1 μg of closed circular plasmid DNA, pDL277, Spec^r (5), was added and the samples were divided into two aliquots, only one of which was supplemented with synthetic CSP (sCSP) (Hospital for Sick Children Biotechnology Services, Toronto, Ontario, Canada) at a final concentration of 750 ng/ml (28). To study genetic competence in the mutant and parent strains, we performed TE assays as described previously (28).

Examination of the *vicK* deficient strain, in vivo, for plaque formation and cariogenic potential. Specific-pathogen-free, caries-susceptible Osborne-Mendel rats (Center for Dental and Oral Medicine and Cranio-Maxillofacial Surgery, Zurich, Switzerland) were used to investigate in vivo effects of the *vicK* deletion on smooth-surface dental plaque and smooth and fissure caries, as well as on the establishment of *S. mutans* in the oral microbiota. Each experimental group consisted of 10 animals. Thirteen days after birth, the animals were transferred to stainless steel screen bottom cages without bedding and fed a finely ground stock diet (diet no. 3433; Provimi Kliba AG). Tap water and food were available ad libitum. On day 20 after birth, the dams were removed and the littermates distributed among the treatment groups (10 rats/group). On days 21 and 22, each rat was infected orally, twice daily, using 200 μl of a heavy bacterial suspension that comprised the parent UA159 strain or the *vicK* deletion mutant. To support the implantation of these bacteria, all rats received drinking water containing 2% sucrose and 2% glucose during days 20 to 22, as well as low-cariogenic diet 2000a (consisting of 28% skim milk, 15% powdered sucrose, 49% wheat flour, 5% brewer's yeast, 2% Gevral protein, and 1% sodium chloride). On day 23 following the association period, sterilization of the feeding and housing equipment was continued. Necessary precautions were taken to avoid cross-contamination and maintain a clean environment. Five days after association with the test strains, swabs were taken from the oral cavities of five rats per treatment group to confirm that the bacteria had become established. Shortly before the end of the study, oral swabs were taken from all 20 rats to obtain a final indication of the microbial status of the animals.

On day 51 (at the end of the 27-day experimental period), the animals were sacrificed. The upper and lower jaws were dissected and immersed in fixative (10% buffered formalin phosphate) for a minimum of 72 h. Erythrosin-stained maxillary molars were evaluated for plaque extent using a method described previously (39). Smooth-surface carious lesions were scored according to Keyes (22), and mandibular molars were sectioned and scored for fissure caries as specified by König et al. (24). The data were analyzed by two-way analysis of variance and least-significant-difference (LSD) tests using the analysis-of-variance statistics program.

Microbiological analyses of rat samples. The swabs taken from each animal were immersed in sterile test tubes containing phosphate-buffered saline and thoroughly shaken. An aliquot was used for culture analyses, and the remaining suspension was immediately frozen. Sample dilutions were plated onto Trypticase yeast Columbia blood (TYCB) agar using a spiral dilutor to obtain total floral counts. Dilutions were also plated onto Trypticase yeast agar supplemented with 20% sucrose and bacitracin to enumerate *S. mutans* bacteria. Both the parental and mutant strains were also plated onto TYCB agar containing 10 μg/ml erythromycin as a control for possible contamination.

RESULTS

Structural organization of the *S. mutans vicRKX* locus. The *S. mutans vicRKX* genes span a region of DNA from 1444056 to 1446908 bp (NCBI) on the minus strand of the *S. mutans* UA159 chromosome (Fig. 1A). The *vicK* coding sequence is 1,350 bp in size and encodes a putative histidine kinase sensor protein with a predicted mass of 51,686 Da (450 amino acids [aa]). A BlastP search revealed that VicK shares high similarity with the *S. pyogenes* VicK protein (NP_268803) and with a putative histidine kinase in *S. pneumoniae* (HK02, NP_358699). The *vicR* coding sequence is 705 bp in size and encodes a putative response regulator protein with a predicted molecular mass of 26,900 Da (235 aa). A BlastP search of VicR revealed that it shared high similarity with the *S. pyogenes* VicR protein (NP_268803.1) and with other response regulators in *S. agalactiae* (NP_687734) and *S. pneumoniae* (NP_606786.1). The *vicX* coding sequence is 801 bp in size and codes for a hypothetical protein with a predicted mass of 29,680 Da (267 aa). A BlastP search indicated that *S. mutans* VicX shares amino acid similarity with VicX in *S. pneumoniae* (NP_345691), VicX in *S. pyogenes* (NP_268804.1), and a metallo-β-lactamase superfamily protein in *S. agalactiae* (NP_687736).

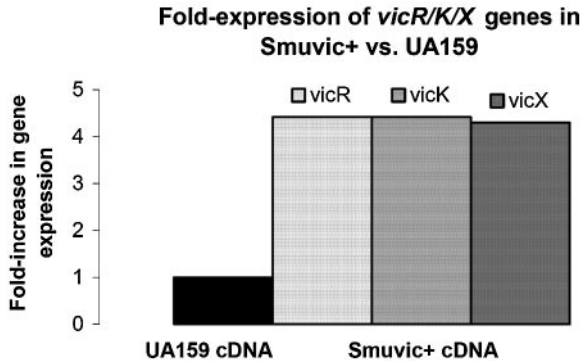

FIG. 2. *S. mutans* UA159 and Smuvic$^+$ cDNAs were used to study expression of the *vicRKX* genes using quantitative rtPCR. For each strain, cDNA samples derived from three independent experiments were subjected to amplification using *vicRKX*-specific primers and *gyrA* primers (normalizing gene). For mutant and wild-type cDNAs, the *n*-fold increase in *vicRKX* expression was calculated relative to that of the UA159 parent, whose expression was set at user-defined value of 1.0.

Confirmation of the *S. mutans vic* mutants. To characterize the putative role of *vicR* and *vicK* in *S. mutans*, we constructed mutations within the *vicRK* coding sequences. The SmuvicK deletion mutation was confirmed by PCR analysis (results not shown). In contrast, we were unable to isolate a *vicR* null mutant. Sequence analysis of transformants revealed the presence of an intact *vicR* gene, as well as chromosomal integration of a VicR fragment that was used to mediate allelic exchange 5′ to the *vicRKX* operon (Table 1). Hence, instead of the expected double-crossover event, the presence of the intact *vicR* gene can be attributed to a Campbell-type crossover event mediated by the circularized a VicR fragment. To assess *vicRK*-specific expression in SmuvicK and Smuvic$^+$ relative to the wild type, we performed rtPCR experiments, the results of which indicated no *vicK*-specific expression in the SmuvicK deletion mutant. rtPCR results for *vic* gene expression are shown in Fig. 2.

***vic* mutants have altered growth rates.** Growth curve analysis of the SmuvicK and Smuvic$^+$ strains revealed altered growth rates compared with that of the UA159 parent strain (Fig. 3). While an overnight culture of UA159 grew as a uniformly turbid cell suspension, SmuvicK and Smuvic$^+$ cells aggregated and accumulated at the bottom of the glass tubes (Fig. 4). Notably, a denser cell aggregate was apparent for the SmuvicK mutant compared with that of Smuvic$^+$. This observation was consistent with growth curves derived from each of three independent experiments that demonstrated a higher growth yield for SmuvicK during stationary phase compared with the wild-type and Smuvic$^+$ strains (Fig. 3). While SmuvicK revealed little difference in the exponential-phase growth rate (mean [min/generation] ± standard error, 59.1 ± 2.6) relative to the wild type (50.1 ± 2), the doubling time of Smuvic$^+$ was greatly increased (78.5 ± 1.5).

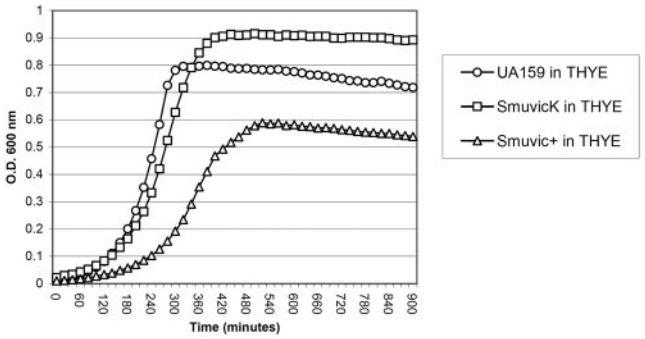

FIG. 3. Growth curves of *S. mutans* UA159, SmuvicK, and Smuvic$^+$ in the presence of THYE. Each datum point is the average of three independent OD values per sample. The results shown are representative of two other independent experiments conducted with the mutant and UA159 parent strains.

Vic mutant strains form aberrant biofilms. Based on biofilms formed on microtiter plates, the mutant biofilms were remarkably different compared with that of the parent (Fig. 4). Specifically, UA159 biofilms presented a smooth and even appearance, whereas SmuvicK and Smuvic$^+$ biofilms appeared rough and clumpy, with the latter seemingly less dense overall. As anticipated, UA159 wild-type cells supplemented with sucrose as the sugar source generated thicker biofilms that were strongly attached to the abiotic surface compared with those generated in glucose-containing medium. In contrast to the wild-type biofilms generated in either glucose or sucrose, growth of SmuvicK in the presence of sucrose gave rise to biofilms that were easily disrupted and only loosely adherent to polystyrene. As shown at the bottom of Fig. 5, relative to the wild-type strain, only a fraction of the SmuvicK cells attached to the surface. However, this easily dispersed phenotype was not apparent when SmuvicK biofilms were formed in glucose-supplemented medium (Fig. 5, top). Closer examination of the SmuvicK biofilm architecture derived from growth in SDM supplemented with glucose revealed areas of densely packed cells interspersed among "open" areas devoid of cells (Fig. 5, top). Notably, closer examination (×5,000 and ×50,000 magnifications) of SmuvicK biofilms derived from growth in diluted 0.25× THYE supplemented with sucrose revealed abnormally long chains of cells that were often detached at the cellular junctions. Compared with the wild type, these mutant cells were generally larger and seemingly associated with a rougher surface that we interpreted as thicker deposits of exopolymer (Fig. 5, bottom). In addition, the Smuvic$^+$ biofilm also revealed aggregated cell clusters that were readily apparent at a magnification of ×1,000.

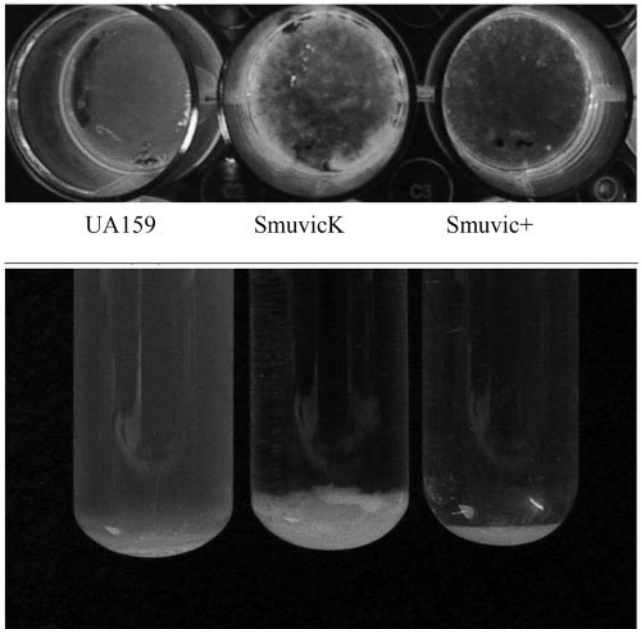

FIG. 4. Biofilm formation (top) and overnight cultures (bottom) of *S. mutans* UA159, SmuvicK, and Smuvic$^+$. Significant phenotypic differences were apparent in the mutant biofilms formed in the presence of modified SDM supplemented with glucose compared to that of the UA159 parent. Overnight cultures of the mutants grown in THYE (containing glucose as the sugar source) resulted in coaggregation of cells.

The *vic* genes affect *S. mutans gtfB*, *gtfC*, *gtfD*, *ftf*, and *gbpB* expression. Since SmuvicK biofilms grown in a sucrose-containing medium were altered in adherence compared with those grown in a medium supplemented with glucose, we hypothesized that the *vic* genes may influence *S. mutans* glucosyltransferase (*gtfB*, *gtfC*, and *gtfD*), fructosyltransferase (*ftf*), and/or *gbpB* expression. To test our hypothesis, we performed quantitative rtPCR using cDNAs derived from SmuvicK, Smuvic$^+$, and UA159 and primers specific for the *gtfB*, *gtfC*, *gtfD*, *ftf*, and *gbpB* genes. Compared with the wild-type parent, the expression of all these genes was increased in the Smuvic$^+$ mutant (Fig. 6). For example, the *gtf* genes were upregulated by more than fivefold in a medium supplemented with either glucose or sucrose (Fig. 6A), whereas *ftf* and *gbpB* expression was increased by nearly fourfold and twofold, respectively (Fig. 6B). In SmuvicK, relative to the wild type, expression of *gtfD* and *gbpB* was reduced, whereas *gtfC* expression remained unchanged (Fig. 6). Notably, in glucose-supplemented medium, expression of *gtfB* showed 3.7-fold more transcript relative to the parent strain.

VicR binds specifically to the promoter regions of *gtfB*, *gtfC*, and *ftf* in vitro. Overproduction of the VicR transcript in Smuvic$^+$ and the concomitant upregulation of the *gtf* genes and *ftf* genes in this mutant suggested that VicR, like many response regulators, might act directly on the promoter regions for these genes. We therefore decided to examine VicR binding to the *gtfBC* and *ftf* promoter regions in vitro. We cloned the *vicR* coding sequence into an expression vector that allowed us to overexpress an amino-terminal MBP-VicR protein fusion. This construct was chosen since similar amino-terminal fusion constructs, like the CovR ortholog in *S. pyogenes*, were shown to bind indistinguishably from native CovR (11). The MBP-*S. mutans* VicR fusion was subsequently purified by >90% as revealed by Coomassie blue staining (data not shown) and used in electrophoretic mobility shift assays. As shown at the top of Fig. 7, MBP-VicR bound the DNA of the promoter regions of *gtfB*, *gtfC*, and *ftf* (MBP purified from the vector alone failed to shift the *gtfB* and *gtfC* promoter regions; data not shown). In electrophoretic mobility shift assay reaction mixtures containing MBP-VicR and *gtfC*, salmon sperm DNA was added in 100-fold excess by weight without diminu-

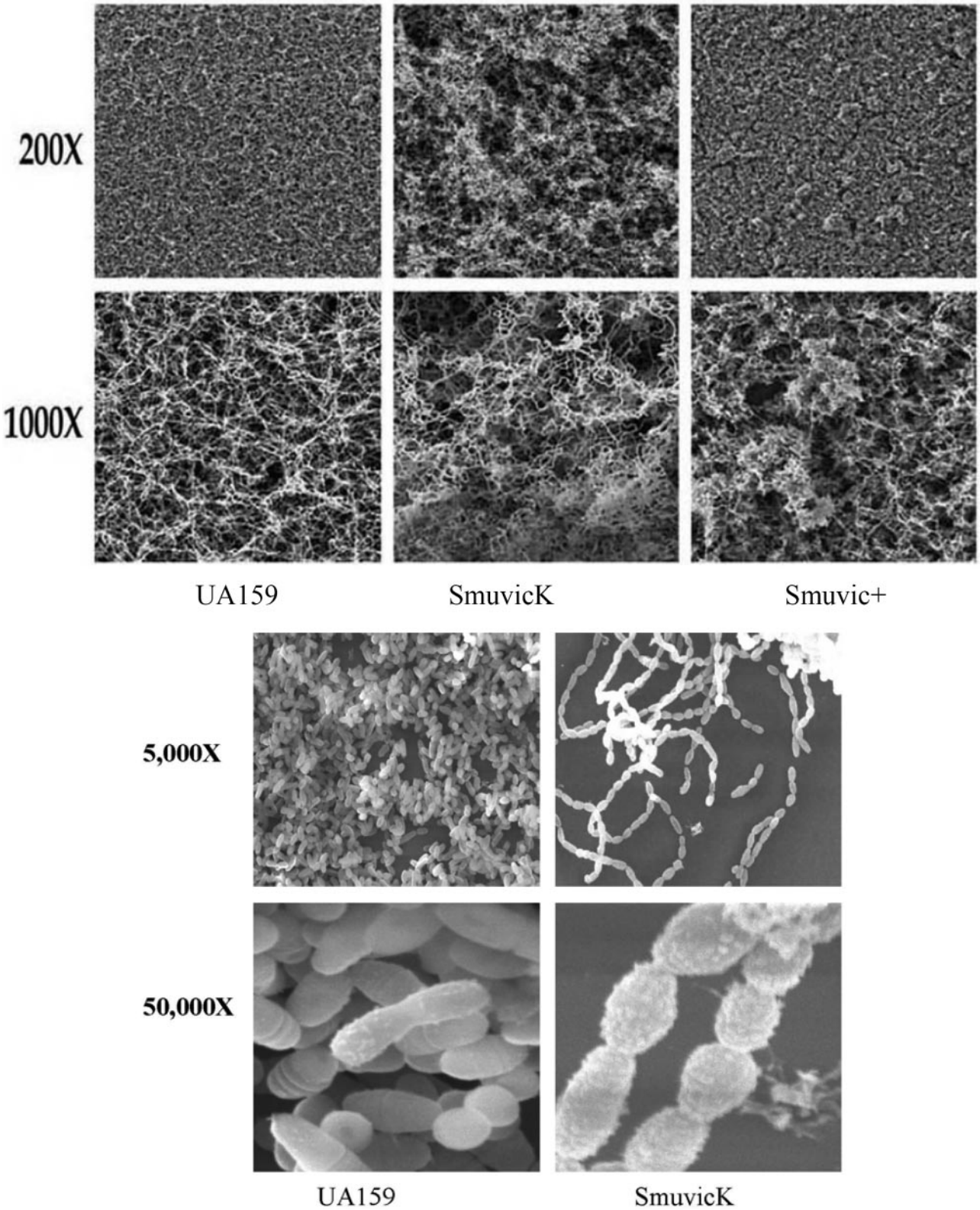

FIG. 5. (Top) SEM of *S. mutans* UA159, SmuvicK, and Smuvic$^+$ developed in SDM supplemented with glucose. (Bottom) SEM of *S. mutans* UA159 and SmuvicK biofilms developed using 0.25× THYE supplemented with 10 mM sucrose.

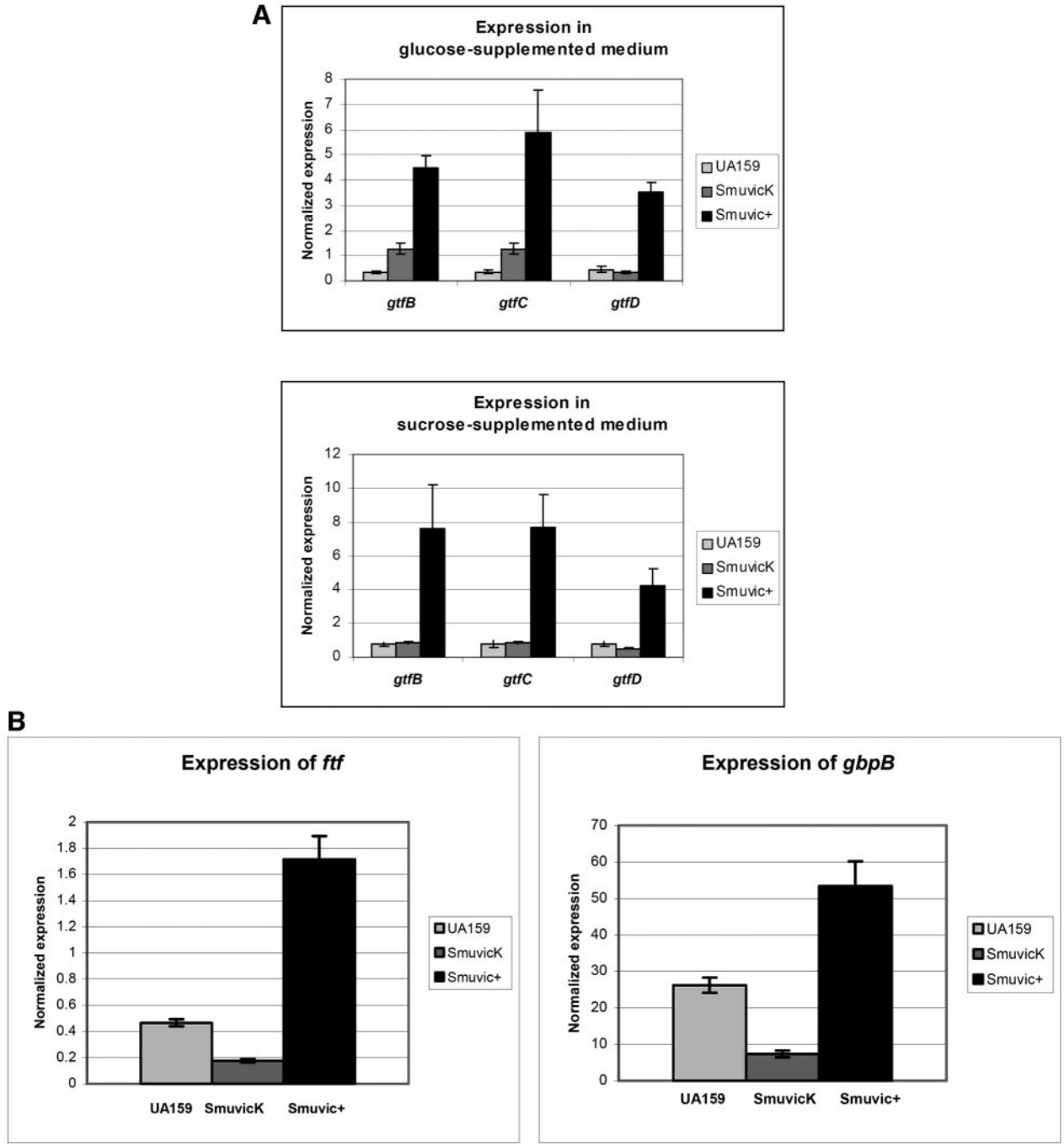

FIG. 6. (A) Expression of *gtfBCD* genes in *S. mutans* UA159, SmuvicK, and Smuvic$^+$ strains. Gene expression was monitored by rtPCR using cDNAs derived from glucose (top)- or sucrose (bottom)-supplemented cultures. Results are the average of three independent experiments conducted using primers specific for the *gtfBCD* genes and *gyrA* (normalizing gene). (B) rtPCR results of *S. mutans* UA159, SmuvicK, and Smuvic$^+$ cDNAs amplified using *S. mutans ftf*- and *gbpB*-specific primers. Each cDNA sample derived from three independent experiments was amplified at least twice using *ftf*, *gbpB*, and *gyrA* (normalizing gene) primers.

tion of the shifted complex. There was, however, a hierarchy of binding. MBP-VicR bound with the highest affinity to the *gtfC* promoter. Although the apparent affinity of MBP-VicR was similar for the *ftf* and *gtfB* promoters, as judged by the proportion of DNA shifted, it was also clear that the shift of the *gtfB* promoter was more distinct and clearly visible, similar to the *ftf* promoter-containing complex. This suggested a greater site specificity of binding. Although we have yet to ascertain the exact sequence that MBP-VicR recognizes, it is likely that there are conserved sequence determinants within the given regions of all three promoter elements. Dubrac and Msadek recently identified a VicR consensus sequence that seems con-

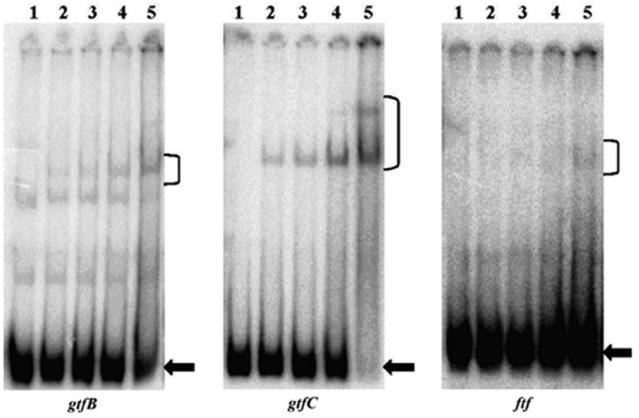

Consensus		TGTWAHNNNNNTGTWAH	
gtfC	-26	TGTTATAAAAGTGTTAC	-10
gtfB	-126	TGTTtTTATCATGTTgT	-110
	-147	TGTTgTTTTTTTGTggg	-138
ftf	-28	TGTTATAAATT*aggattataa*TGTAAC	-2

FIG. 7. (Top) Gel mobility shift assays. DNA-binding reaction mixtures were prepared with end-labeled DNA fragments for the 5′-proximal region of *gtfB*, *gtfC*, or *ftf* and purified MBP-VicR. Lanes 1, no protein; lanes 2, 100 nM; lanes 3, 200 nM; lanes 4, 500 nM; lanes 5, 1,000 nM MBP-VicR. The calculated shifts for each substrate in order of 100 to 1,000 were as follows: GtfB, 0.42, 3.69, 5.28, and 24.79%; GtfC, 6.46, 7.62, 23.08, and 93.69%; Ftf, 1.96, 2.43, 7.65, and 19.19%. All values were calculated using Image Quant 5.0 software from Molecular Dynamics. Brackets indicate protein-DNA complex, arrows indicate free DNA. (Bottom) Putative VicR binding sequences based on the *Bacillus*/*Streptococcal* VicR consensus sequences (11, 21). Numbers preceding and following each sequence represent the distance from the transcriptional start for each gene. W is A or T, H represents anything except G, and mismatches are in lowercase. Lowercase italics represent an extra 10 bp between the hexamers.

served across many gram-positive genera (9). As shown at the bottom of Fig. 7, the sequence TGTWAHNNNNNTGTWAH (where W is A or T and H is A, T, or C) was perfectly conserved in the *gtfC* promoter, partially conserved in the *gtfB* promoter (although there are several possible iterations), and found perfectly conserved in the *ftf* promoter but with the important caveat that there was an additional 10 bp or helical repeat that separated the more conserved hexamers.

The *vic* mutants affect extracellular polysaccharide formation. Since the biofilm architecture and adhesive properties are affected by mutagenesis of the *vic* genes, we sought to gain insight into the synthesis of extracellular polysaccharides in SmuvicK, Smuvic$^+$, and their parent UA159 strain. Based on the results of three independent experiments, cell-free supernatants of SmuvicK cultures resulted in a negative value for the percentage increase in ^{14}C incorporated into dextran, possibly the result of degradation or removal of the newly synthesized dextran during the methanol washes (Fig. 8). In contrast, the rate of extracellular polysaccharide formation by Smuvic$^+$ culture supernatants was increased relative to the wild type.

The *vic* mutants have altered transformation efficiencies. Genetic competence assays indicated that SmuvicK and Smuvic$^+$ have altered TE compared to the UA159 wild-type progenitor strain, thereby supporting a role for the *vic* gene products in competence development. In the absence of CSP, the TE of Smuvic$^+$ was reduced by approximately 100-fold compared with the wild type, whereas the SmuvicK TE was not remarkably different from that of the wild type (data not shown). While addition of sCSP markedly increased the transformability of the wild-type strain by nearly 1,000-fold, the TEs of SmuvicK and Smuvic$^+$ were only increased by approximately 20- and 88-fold, respectively (Fig. 9). In other words, the percent change in TE (with added CSP) decreased by 60-fold ($n = 5$) and 13-fold ($n = 3$) for SmuvicK and Smuvic$^+$, respectively.

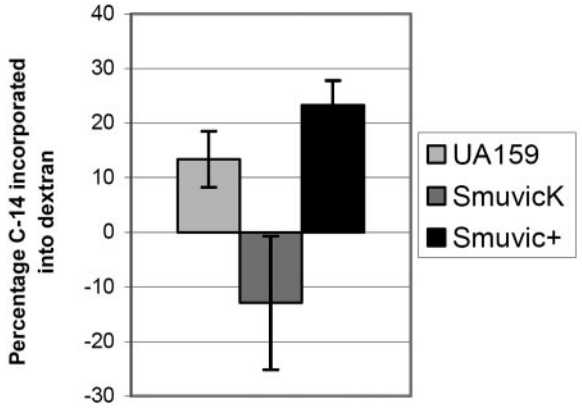

FIG. 8. EPS by SmuvicK, Smuvic$^+$, and their UA159 progenitor strain. Results shown are the averages of three independent experiments conducted to monitor the percentage of ^{14}C incorporated into dextran following 30 min of incubation.

SmuvicK is significantly increased in surface plaque formation and reduced in CFU count in vivo. Compared with the UA159 parent strain, SmuvicK was significantly increased in its ability to form smooth-surface plaque (PF, <0.001; Table 3) in a specific-pathogen-free rat model. However, the development of initial dentinal T lesions, advanced dentinal fissure lesions,

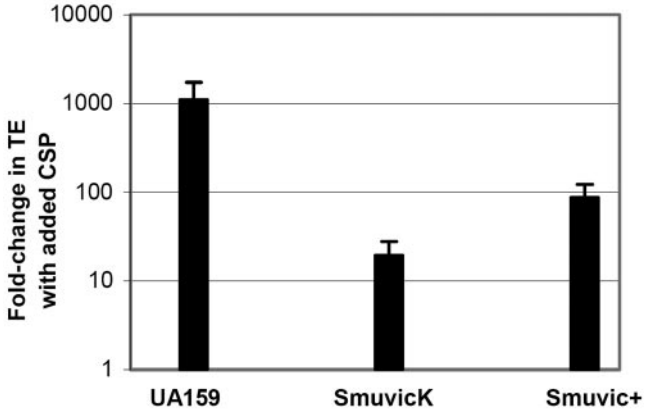

FIG. 9. *n*-fold increases in transformation efficiencies of *S. mutans* UA159, SmuvicK, and Smuvic$^+$ strains when supplemented with sCSP. TE of cultures without addition of CSP was set at a user-defined value of 1.0. The abilities of SmuvicK and Smuvic$^+$ to respond to the signal peptide were impaired by nearly 60- and 13-fold, respectively, compared to the UA159 parent.

TABLE 3. Mean (per rat) smooth-surface plaque extent, initial and advanced dentinal fissure lesions, and smooth-surface caries[a]

Treatment group[b] or parameters	Plaque extent (Δ)	Initial dentinal fissure lesions (ΔΔ)	Advanced dentinal fissure lesions (ΔΔ)	Smooth-surface caries (ΔΔΔ)
UA159	1.0 ± 0.00	9.2 ± 1.55	4.4 ± 2.17	0.9 ± 1.29
SmuvicK	2.5 ± 0.53[c]	8.8 ± 1.40[d]	5.1 ± 1.52[d]	1.1 ± 1.37[d]
PF	<0.001	<0.001	<0.001	<0.001
LSD, 0.001	0.67	1.94	2.78	2.63

[a] Symbols: Δ, 4 U at risk; ΔΔ, 12 fissures at risk; ΔΔΔ, 20 U at risk.
[b] There were 10 rats in each treatment group.
[c] LSD, 0.001.
[d] No statistically significant difference.

and smooth-surface caries lesions were not significantly altered in the *vicK*-deficient mutant compared with the parent (Table 3). Although growth of SmuvicK and UA159 in blood agar was significantly different at a confidence interval of 95%, there were no significant differences in the total number of CFU between these strains in samples derived from rats (Table 4). While there was no visible growth of the parent strain on TYCB plates supplemented with erythromycin, data collected from TYCB plates without erythromycin revealed a significant reduction in CFU counts for SmuvicK compared with the parent strain (PF, <0.001; Table 4).

DISCUSSION

The aim of this study was to investigate the VicRK signal transduction system and its effects on various virulence attributes of *S. mutans*. Similar to its ortholog in *S. pneumoniae*, *S. mutans* VicR seems essential for the viability of this bacterium. Based on our findings, the *vic* gene products appear to modulate adherence, biofilm formation, and genetic competence development in *S. mutans*. Notably, they regulate the expression of several virulence-associated genes affecting synthesis and adhesion to polysaccharides, including *gtfBCD*, *ftf*, and *gbpB*. Moreover, studies conducted utilizing the *vicK*-deficient mutant in specific-pathogen-free rats revealed a significant increase in smooth-surface plaque compared with the wild-type UA159 parent, whereas the incidence of dental caries was not affected.

The VicRK signal transduction system in *S. mutans* was recently mentioned in a study by Bhagwat et al. in which construction of a *vicR* knockout mutant proved to be futile (4). We experienced the same outcome when repeated attempts to construct an *S. mutans vicR* null mutation in the UA159 and NG8 wild-type strains resulted in loss of viability. Consistent with this finding is a report by Wagner et al. that indicated an inability to generate a deletion mutation in the *S. pneumoniae vicR* ortholog (46). Yet, Lee et al. recently published a report claiming to have inactivated the *S. mutans vicR* gene, called *covR* in their paper (26). Upon obtaining this mutant and examining the cDNAs generated from its RNA pool using three different primer sets that flank the *vicR* coding sequence, we noted transcription of the *vicR* gene at levels that were comparable to that of the parent (results not shown). In fact, if one examines the predicted integration site in the report of Lee et al., it is evident that the map of the locus shows insertion of the mutagenic construct 5′ proximal to the wild-type *covR* (*vicR*) gene. During our attempted mutagenesis of *vicR*, we were unable to demonstrate that *vicR* is absolutely required for viability. However, it is reasonable to assume that the *vicR* gene plays a vital role that is essential for the survival of *S. mutans* under our laboratory conditions. Transformants obtained during the mutagenesis of *vicR* showed overexpression of the *vicRKX* genes likely resulting from a promoter duplication caused by a Campbell-type insertion of the circularized VicR fragment. In contrast, *S. mutans* viability was not affected when *vicK* was disrupted. Hence, the phenotypic differences that we observed for SmuvicK and Smuvic$^+$, which include adhesion, biofilm formation, and TE, can probably be attributed to their genotypic differences, although intercellular interactions involving cross talk between VicRKX and other signal transduction systems cannot be discounted.

TABLE 4. Mean (per rat) total flora on Columbia blood agar plates and CFU counts on TYCB plates containing bacitracin with and without erythromycin

Treatment group[a] or parameter	Total flora on Columbia blood agar	CFU count on TYCB (10^6)	
		With erythromycin	Without erythromycin
UA159	29.8 ± 18.2	0.0 ± 0.00	15.7 ± 12.80
SmuvicK	21.5 ± 25.00[b]	0.7 ± 0.38	0.7 ± 0.38[c]
PF	<0.05		<0.001
LSD, 0.001			12.50

[a] There were 10 rats per group.
[b] Not statistically significant difference.
[c] LSD, 0.001.

The ability of *S. mutans* to colonize teeth is paramount to the initiation and progression of dental caries. Among the *S. mutans* surface-associated proteins that facilitate adherence and colonization are glucosyltransferases (GtfB, GtfC, and GtfD) and a fructosyltransferase (Ftf), which catalyze the cleavage of sucrose to synthesize extracellular glucan and fructan polymers, respectively (2, 16, 17, 19, 38, 41). GtfB and GtfC produce water-insoluble glucans, which function as adhesive molecules that anchor bacteria to the tooth pellicle (13, 36). Oral bacterial aggregation is also mediated by interactions between surface-associated glucan-binding proteins (Gbp) that adhere to glucans, thereby promoting plaque formation (33). Collectively, these enzymes serve an important role in the pathogenicity of *S. mutans*. For instance, rats harboring *S. mutans gtfBCD*- or *ftf*-deficient mutants proved to be hypocariogenic (6, 35, 41, 47). Also, systemic or mucosal immunization with GbpB was shown to induce protective immunity against dental

caries in rats, indicating that GbpB may be an important target for the development of caries vaccines (42). In this study, we analyzed biofilms formed by *vic* mutants using SEM and visual examination of biofilms grown in microtiter plates. In sucrose-supplemented medium, we noticed that biofilms formed using UA159 wild-type cells were thicker and firmly attached to the surface, in contrast to those developed in the presence of glucose. In contrast, SmuvicK biofilms that formed in the presence of sucrose as the sugar source were loosely attached to the abiotic surface and easily disrupted compared with those derived from a glucose-supplemented medium, as well as wild-type biofilms derived from glucose- or sucrose-containing medium. Therefore, our findings support *vicRK* as a regulator of sucrose-mediated adherence in *S. mutans*. We henceforth conducted quantitative rtPCR experiments to assess the expression of *gtfBCD*, *ftf*, and *gbpB* in SmuvicK and Smuvic$^+$ cells grown in glucose- and/or sucrose-containing medium. Our results indicated that *vicK* acts as a positive regulator of *ftf*, *gtfD*, and *gbpB* expression. In the presence of sucrose, increased expression of the *gtfBC* genes was observed only in the *vic*-overexpressing mutant. The down-regulation of the *ftf*, *gtfD*, and *gbpB* genes can possibly account for the easily detachable biofilm phenotype of the *vicK*-deficient mutant as a result of a reduction in its rate of total dextran formation. The EPS assay is indicative of the rate of formation of extracellular glucans and fructans produced by the activity of Gtf proteins and Ftf on sucrose but does not, however, differentiate between soluble and insoluble polymers. Repeated measurements of the rate of dextran formation in SmuvicK resulted in negative values. It is possible that the type of dextran formed by this mutant is degraded or easily disturbed and removed during the methanol washes in the EPS assay protocol. In their publication, Lee et al. reported that CovR (VicR) negatively regulated glucose- and glucuronic acid-containing carbohydrate production (26). Although the CovR (VicR) mutant described by Lee et al. produced a *covR* transcript, their complementation studies conducted by supplying the mutant with multiple copies of the gene on a plasmid affected the proportion of glucose- and glucuronic acid-containing EPS, suggesting a relationship between this TCSTS and the type and proportion of EPS produced by *S. mutans*.

Since studying oral bacteria in their natural mode of growth (biofilms) is of enormous significance to understanding pathogenetic mechanisms, we sought to gain insight into the contribution of the *vic* genes in the formation of *S. mutans* biofilms. Relative to biofilms formed by the UA159 wild-type parent strain, the mutant biofilms showed altered architecture as judged by visual inspection of biofilms on microtiter plates and by SEM. Specifically, compared with wild-type biofilms that appeared smooth and composed of uniformly distributed streptococcal chains and intracellular spaces, mutant biofilms seemed to clump and to form cellular aggregates. SmuvicK biofilms demonstrated the highest variability, with cellular aggregates emerging from relatively large open areas devoid of cells. Some of the streptococcal chains appeared "curly" (Fig. 5, top), the likely result of aberrant cell division or abnormal carbohydrate polymer deposition at the cell surface. Its chains were unusually long and seemed disconnected at the cell junctions (Fig. 5, bottom), probably contributing to their easily disruptable biofilm phenotype. Similar to SmuvicK, Smuvic$^+$ exhibited cell aggregates that projected outward in the shape of circular mounds from an otherwise evenly distributed biofilm architecture. Recently, Ng et al. demonstrated that the VicRK TCSTS in *S. pneumoniae* positively regulates expression of PcsB (37). PcsB acts as a cell wall hydrolase, and downregulation of PcsB results in defects in cell separation, synthesis, and morphology (37). Interestingly, the PcsB homolog in *S. mutans* is GbpB, which is positively regulated by the *vic* genes. Hence, if *gbpB* in *S. mutans* serves a similar function, the long streptococcal chains that seemed disconnected at cell junctions in the *vicK*-deficient mutant may be possibly caused by the down-regulation of *gbpB* in this mutant. Additional studies are warranted not only to understand the role of the *vicR* and *vicX* genes in regulating the expression of *gbpB* in *S. mutans* but also to define the role of *gbpB* as a cell wall hydrolase in *S. mutans*.

In reference to VicR, the results of the in vitro binding studies supported the interaction of MBP-VicR with the promoters of *gtfB*, *gtfC*, and *ftf*. While we were able to demonstrate VicR specificity for these regions, we have yet to identify the specific DNA sequences to which VicR binds. Dubrac and Msadek have described a consensus that accommodates our hierarchy of binding (9). In addition to providing a consensus consisting of a conserved hexamer separated by five nonspecific nucleotides, they demonstrated that at extremely high concentrations, the VicR homolog of *Staphylococcus aureus* can even bind to a single hexamer. According to our model, each conserved hexamer is recognized by a single VicR monomer and hence binding at a site with properly spaced hexamers, like *gtfC*, actually occurs as a homodimer. In the case of the *ftf* promoter sequence, we would argue that the active species is actually a dimer of dimers. Since the hexamers are in direct repeat with the first T's 11 bp apart, it is possible to have cooperative interactions and hence oligomerization, which has been observed for NtrC (48). Since TCSTS response regulators are typically regulated by their cognate histidine kinase, future experiments will need to examine the role of the phosphorylation state of VicR in DNA binding. We do not know the state of phosphorylation of the MBP-VicR fusion protein, nor do we know the effects of the presence of the amino-terminal fusion protein. This leaves us with a conundrum, as the consensus sequences actually overlap the promoters themselves. Since we have seen stimulation of *gtfB*, *gtfC*, and *ftf* transcription in the VicR overproducer, it stands to reason that transcription is enhanced by VicR binding to these promoters. Although the mechanism is unclear, there is a precedent. Lantibiotics are often self-regulated through a TCSTS quorum-sensing system. According to the model, as the lantibiotic concentration increases extracellularly, it binds to its cognate histidine kinase, resulting in phosphorylation of its partnered response regulator. Similar to our observations, the putative response regulator binding sites overlap the promoter regions of select genes just upstream of the −10 region (23). The specifics of this mechanism are unknown but clearly common among bacteria. Future experiments will focus on finer biochemical analysis of the VicR DNA binding interactions, including footprinting experiments that should identify the binding site.

In accordance with SmuvicK aberrant biofilm formation is the variant smooth-surface dental plaque content and CFU count noted for this mutant in vivo relative to the wild type.

However, despite an increase in smooth-surface plaque, SmuvicK was not hypercariogenic in a specific-pathogen-free animal model relative to the wild type. One possibility is that the SmuvicK biofilm was easily disrupted, thereby reducing the virulence potential usually associated with increased smooth-surface plaque. Supporting this argument is the diminished SmuvicK viable count observed for this mutant on TYCB agar that was supplemented with bacitracin. Alternatively, one might speculate that the SmuvicK adherence defect was masked in vivo by the presence of other oral microbes that could have "nonspecifically" coaggregated with the mutant, anchoring it to the tooth surface. It is important to note that the main factors that affect cariogenicity include the microbial composition, the diet, and the nature of the polysaccharide matrix, which determines the diffusion properties of plaque. Hence, in reference to polymer production in SmuvicK, excess plaque extent or volume would not necessarily result in hypercariogenicity. Among other phenotypes observed for the *vic* mutants were alterations in genetic competence development in the presence or absence of CSP. The results of our experiments indicate that the efficiency with which *S. mutans* can take up foreign DNA is indeed affected by the products of the *vic* genes. In the absence of CSP, we observed that the TE for Smuvic$^+$ was decreased by approximately 100-fold compared with the parent strain, whereas the TE was not necessarily altered in SmuvicK. The addition of CSP failed to increase the TE of either mutant to levels observed for the wild-type cells (Fig. 9). Previously, we described a *comCDE* quorum-sensing system in *S. mutans* that induces genetic competence (28). The *comCDE* genes encode the precursor CSP (ComC), its sensor protein (ComD), and a cognate response regulator (ComE). The absence of any one of these genes compromises TE. The reliance of the *comCDE* system on SmuvicK to restore the CSP-dependent wild-type TE levels suggests that the *S. mutans vicK*-initiated signal transduction system has a distinct regulatory effect on the competence development pathway. Although it is possible that VicK might act as a receptor for CSP in addition to ComD, this needs to be examined directly to test this assumption.

In summary, this work provides significant insight into important regulatory functions of the *vicRK* signal transduction system in *S. mutans*. However, more studies are warranted to define the downstream target genes that are regulated by this signaling pathway and the *vicX* gene. Deciphering the molecular mechanism(s) that underlies the *vicRK* signaling system in this oral pathogen can foster our understanding of virulence gene regulation in *S. mutans* and so reveal novel targets for therapeutics directed against *S. mutans* cariogenicity.

ACKNOWLEDGMENTS

We thank Robert Chernecky for the SEM, Richard Mair and Peter Lau for assistance with bioinformatic analyses, and Song F. Lee for kindly providing the *vicR* (*covR*) mutant strain of *S. mutans* NG8.

This study was supported by NIH grant RO1DE013230 and CIHR grant MT-15431 to D.G.C., NIH grant R01DE013965 to S.D.G., and NIH grant R15DE014854 to G.A.S. D.G.C. is a recipient of a Canada Research Chair. M.D.S. is a CIHR Strategic Training Fellow supported by training grant STP-53877 and a Harron Scholarship.

REFERENCES

1. **Ajdic, D., W. M. McShan, R. E. McLaughlin, G. Savic, J. Chang, M. B. Carson, C. Primeaux, R. Tian, S. Kenton, H. Jia, S. Lin, Y. Qian, S. Li, H. Zhu, F. Najar, H. Lai, J. White, B. A. Roe, and J. J. Ferretti.** 2002. Genome sequence of *Streptococcus mutans* UA159, a cariogenic dental pathogen. Proc. Natl. Acad. Sci. USA **99:**14434–14439.
2. **Aoki, H., T. Shiroza, M. Hayakawa, S. Sato, and H. K. Kuramitsu.** 1986. Cloning of a *Streptococcus mutans* glucosyltransferase gene coding for insoluble glucan synthesis. Infect. Immun. **53:**587–594.
3. **Armitage, J. P.** 1999. Bacterial tactic responses. Adv. Microb. Physiol. **41:** 229–289.
4. **Bhagwat, S. P., J. Nary, and R. A. Burne.** 2001. Effects of mutating putative two-component systems on biofilm formation by *Streptococcus mutans* UA159. FEMS Microbiol. Lett. **205:**225–230.
5. **Buckley, N. D., L. N. Lee, and D. J. LeBlanc.** 1995. Use of a novel mobilizable vector to inactivate the *scrA* gene of *Streptococcus sobrinus* by allelic replacement. J. Bacteriol. **177:**5028–5034.
6. **Burne, R. A., Y. Y. Chen, D. L. Wexler, H. Kuramitsu, and W. H. Bowen.** 1996. Cariogenicity of *Streptococcus mutans* strains with defects in fructan metabolism assessed in a program-fed specific-pathogen-free rat model. J. Dent. Res. **75:**1572–1577.
7. **Cvitkovitch, D. G.** 2001. Genetic competence and transformation in oral streptococci. Crit. Rev. Oral Biol. Med. **12:**217–243.
8. **Davies, D. G., M. R. Parsek, J. P. Pearson, B. H. Iglewski, J. W. Costerton, and E. P. Greenberg.** 1998. The involvement of cell-to-cell signals in the development of a bacterial biofilm. Science **280:**295–298.
9. **Dubrac, S., and T. Msadek.** 2004. Identification of genes controlled by the essential YycG/YycF two-component system of *Staphylococcus aureus*. J. Bacteriol. **186:**1175–1181.
10. **Fabret, C., and J. A. Hoch.** 1998. A two-component signal transduction system essential for growth of *Bacillus subtilis*: implications for anti-infective therapy. J. Bacteriol. **180:**6375–6383.
11. **Federle, M. J., and J. R. Scott.** 2002. Identification of binding sites for the group A streptococcal global regulator CovR. Mol. Microbiol. **43:**1161–1172.
12. **Fukuchi, K., Y. Kasahara, K. Asai, K. Kobayashi, S. Moriya, and N. Ogasawara.** 2000. The essential two-component regulatory system encoded by *yycF* and *yycG* modulates expression of the *ftsAZ* operon in Bacillus subtilis. Microbiology **146**(Pt. 7)**:**1573–1583.
13. **Hamada, S., and H. D. Slade.** 1980. Biology, immunology, and cariogenicity of *Streptococcus mutans*. Microbiol. Rev. **44:**331–384.
14. **Hamilton, I. R., and N. D. Buckley.** 1991. Adaptation by *Streptococcus mutans* to acid tolerance. Oral Microbiol. Immunol. **6:**65–71.
15. **Hamilton, I. R., and G. Svensater.** 1998. Acid-regulated proteins induced by *Streptococcus mutans* and other oral bacteria during acid shock. Oral Microbiol. Immunol. **13:**292–300.
16. **Hanada, N., and H. K. Kuramitsu.** 1988. Isolation and characterization of the *Streptococcus mutans gtfC* gene, coding for synthesis of both soluble and insoluble glucans. Infect. Immun. **56:**1999–2005.
17. **Hanada, N., and H. K. Kuramitsu.** 1989. Isolation and characterization of the *Streptococcus mutans gtfD* gene, coding for primer-dependent soluble glucan synthesis. Infect. Immun. **57:**2079–2085.
18. **Hanna, M. N., R. J. Ferguson, Y. H. Li, and D. G. Cvitkovitch.** 2001. *uvrA* is an acid-inducible gene involved in the adaptive response to low pH in *Streptococcus mutans*. J. Bacteriol. **183:**5964–5973.
19. **Honda, O., C. Kato, and H. K. Kuramitsu.** 1990. Nucleotide sequence of the *Streptococcus mutans gtfD* gene encoding the glucosyltransferase-S enzyme. J. Gen. Microbiol. **136:**2099–2105.
20. **Howell, A., S. Dubrac, K. K. Andersen, D. Noone, J. Fert, T. Msadek, and K. Devine.** 2003. Genes controlled by the essential YycG/YycF two-component system of *Bacillus subtilis* revealed through a novel hybrid regulator approach. Mol. Microbiol. **49:**1639–1655.
21. **Idone, V., S. Brendtro, R. Gillespie, S. Kocaj, E. Peterson, M. Rendi, W. Warren, S. Michalek, K. Krastel, D. Cvitkovitch, and G. Spatafora.** 2003. Effect of an orphan response regulator on *Streptococcus mutans* sucrose-dependent adherence and cariogenesis. Infect. Immun. **71:**4351–4360.
22. **Keyes, P. H.** 1958. Dental caries in the molar teeth of rats. Distribution of lesions induced by high-carbohydrate low-fat diets. J. Dent. Res. **37:**1077–1087.
23. **Kleerebezem, M., and L. E. Quadri.** 2001. Peptide pheromone-dependent regulation of antimicrobial peptide production in gram-positive bacteria: a case of multicellular behavior. Peptides **22:**1579–1596.
24. **König, K. G., T. M. Marthaler, and H. R. Muhlemann.** 1958. Methodik der kurzfristig erzeugten Rattenkaries. Dtsch. Zahn- Mund- Kieferheilkd. **29:** 99–127.
25. **Lau, P. C., C. K. Sung, J. H. Lee, D. A. Morrison, and D. G. Cvitkovitch.** 2002. PCR ligation mutagenesis in transformable streptococci: application and efficiency. J. Microbiol. Methods **49:**193–205.
26. **Lee, S. F., G. D. Delaney, and M. Elkhateeb.** 2004. A two-component *covRS* regulatory system regulates expression of fructosyltransferase and a novel extracellular carbohydrate in *Streptococcus mutans*. Infect. Immun. **72:**3968–3973.
27. **Li, Y. H., M. N. Hanna, G. Svensater, R. P. Ellen, and D. G. Cvitkovitch.** 2001. Cell density modulates acid adaptation in *Streptococcus mutans*: implications for survival in biofilms. J. Bacteriol. **183:**6875–6884.
28. **Li, Y. H., P. C. Lau, J. H. Lee, R. P. Ellen, and D. G. Cvitkovitch.** 2001.

Natural genetic transformation of *Streptococcus mutans* growing in biofilms. J. Bacteriol. **183:**897–908.
29. **Li, Y. H., P. C. Lau, N. Tang, G. Svensater, R. P. Ellen, and D. G. Cvitkovitch.** 2002. Novel two-component regulatory system involved in biofilm formation and acid resistance in *Streptococcus mutans*. J. Bacteriol. **184:** 6333–6342.
30. **Li, Y. H., N. Tang, M. B. Aspiras, P. C. Lau, J. H. Lee, R. P. Ellen, and D. G. Cvitkovitch.** 2002. A quorum-sensing signaling system essential for genetic competence in *Streptococcus mutans* is involved in biofilm formation. J. Bacteriol. **184:**2699–2708.
31. **Loesche, W. J.** 1986. Role of *Streptococcus mutans* in human dental decay. Microbiol. Rev. **50:**353–380.
32. **Loo, C. Y., D. A. Corliss, and N. Ganeshkumar.** 2000. *Streptococcus gordonii* biofilm formation: identification of genes that code for biofilm phenotypes. J. Bacteriol. **182:**1374–1382.
33. **Mattos-Graner, R. O., S. Jin, W. F. King, T. Chen, D. J. Smith, and M. J. Duncan.** 2001. Cloning of the *Streptococcus mutans* gene encoding glucan binding protein B and analysis of genetic diversity and protein production in clinical isolates. Infect. Immun. **69:**6931–6941.
34. **McDermid, A. S., A. S. McKee, D. C. Ellwood, and P. D. Marsh.** 1986. The effect of lowering the pH on the composition and metabolism of a community of nine oral bacteria grown in a chemostat. J. Gen. Microbiol. **132:**1205–1214.
35. **Munro, C., S. M. Michalek, and F. L. Macrina.** 1991. Cariogenicity of *Streptococcus mutans* V403 glucosyltransferase and fructosyltransferase mutants constructed by allelic exchange. Infect. Immun. **59:**2316–2323.
36. **Nakano, Y. J., and H. K. Kuramitsu.** 1992. Mechanism of *Streptococcus mutans* glucosyltransferases: hybrid-enzyme analysis. J. Bacteriol. **174:**5639–5646.
37. **Ng, W. L., K. M. Kazmierczak, and M. E. Winkler.** 2004. Defective cell wall synthesis in *Streptococcus pneumoniae* R6 depleted for the essential PcsB putative murein hydrolase or the VicR (YycF) response regulator. Mol. Microbiol. **53:**1161–1175.
38. **Pucci, M. J., K. R. Jones, H. K. Kuramitsu, and F. L. Macrina.** 1987. Molecular cloning and characterization of the glucosyltransferase C gene (*gtfC*) from *Streptococcus mutans* LM7. Infect. Immun. **55:**2176–2182.
39. **Regolati, B., and P. Hotz.** 1972. Cariostatic effect of glycerophosphate. Helv. Odontol. Acta **16:**13–18.
40. **Sato, Y., Y. Yamamoto, and H. Kizaki.** 2000. Construction of region-specific partial duplication mutants (merodiploid mutants) to identify the regulatory gene for the glucan-binding protein C gene *in vivo* in *Streptococcus mutans*. FEMS Microbiol. Lett. **186:**187–191.
41. **Schroeder, V. A., S. M. Michalek, and F. L. Macrina.** 1989. Biochemical characterization and evaluation of virulence of a fructosyltransferase-deficient mutant of *Streptococcus mutans* V403. Infect. Immun. **57:**3560–3569.
42. **Smith, D. J., and M. A. Taubman.** 1996. Experimental immunization of rats with a *Streptococcus mutans* 59-kilodalton glucan-binding protein protects against dental caries. Infect. Immun. **64:**3069–3073.
43. **Stein, T., S. Borchert, P. Kiesau, S. Heinzmann, S. Kloss, C. Klein, M. Helfrich, and K. D. Entian.** 2002. Dual control of subtilin biosynthesis and immunity in *Bacillus subtilis*. Mol. Microbiol. **44:**403–416.
44. **Stock, A. M., V. L. Robinson, and P. N. Goudreau.** 2000. Two-component signal transduction. Annu. Rev. Biochem. **69:**183–215.
45. **Strauch, M. A., and J. A. Hoch.** 1993. Signal transduction in *Bacillus subtilis* sporulation. Curr. Opin. Genet. Dev. **3:**203–212.
46. **Wagner, C., A. Saizieu Ad, H. J. Schonfeld, M. Kamber, R. Lange, C. J. Thompson, and M. G. Page.** 2002. Genetic analysis and functional characterization of the *Streptococcus pneumoniae vic* operon. Infect. Immun. **70:** 6121–6128.
47. **Yamashita, Y., W. H. Bowen, R. A. Burne, and H. K. Kuramitsu.** 1993. Role of the *Streptococcus mutans gtf* genes in caries induction in the specific-pathogen-free rat model. Infect. Immun. **61:**3811–3817.
48. **Yang, X. F., Y. Ji, B. L. Schneider, and L. Reitzer.** 2004. Phosphorylation-independent dimer-dimer interactions by the enhancer-binding activator NtrC of Escherichia coli: a third function for the C-terminal domain. J. Biol. Chem. **279:**36708–36714.